

Design of AT-DMB Baseband Receiver SoC

Joohyun Lee, Hyuk Kim, Jinkyu Kim, Bontae Koo, Nakwoong Eum, and Hyuckjae Lee

This paper presents the design of an advanced terrestrial digital multimedia broadcasting (AT-DMB) baseband receiver SoC. The AT-DMB baseband is incorporated into a hierarchical modulation scheme consisting of high priority (HP) and low priority (LP) stream decoders. The advantages of the hierarchical modulation scheme are backward compatibility and an enhanced data rate. The structure of the HP stream is the same as that of the conventional T-DMB system; therefore, a conventional T-DMB service is possible by decoding multimedia data in an HP stream. An enhanced data rate can be achieved by using both HP and LP streams. In this paper, we also discuss a time deinterleaver that can deinterleave data for a time duration of 384 ms or 768 ms. The interleaving time duration is chosen using the LP symbol mapping scheme. Furthermore, instead of a Viterbi decoder, a turbo decoder is adopted as an inner error correction system to mitigate the performance degradation due to a smaller symbol distance in a hierarchically modulated LP symbol. The AT-DMB baseband receiver SoC is fabricated using 0.13 μm technology and shows successful operation with a 50 mW power dissipation.

Keywords: AT-DMB, advanced T-DMB, DMB, baseband SoC, hierarchical modulation.

Manuscript received Apr. 27, 2009; revised July 24, 2009; accepted Aug. 6, 2009.

This work was supported by the Ministry of Knowledge Economy of Korea under the title of "Development of advanced transmission technology for the terrestrial DMB system."

Joohyun Lee (phone: +82 42 860 6574, juehyun@etri.re.kr), Hyuk Kim (email: haggyl@etri.re.kr), Jinkyu Kim (email: kimjk@etri.re.kr), Bontae Koo (email: koobt@etri.re.kr), and Nakwoong Eum (email: nweum@etri.re.kr) are with the Convergence Components & Materials Research Laboratory, ETRI, Daejeon, Rep. of Korea.

Hyuckjae Lee (email: hjlee314@kaist.ac.kr) is with the Electrical Engineering Department, KAIST, Daejeon, Rep. of Korea.

doi:10.4218/etrij.09.1209.0009

I. Introduction

Terrestrial digital multimedia broadcasting (T-DMB) [1], [2] service has already been commercially launched in Korea and is becoming a popular broadcasting service among mobile equipment users. Consequently, the T-DMB receiver component is very common to most mobile phone or car-navigation systems. However, the maximum data rate of a T-DMB system is only 1,592 kbps [3], which is just enough for small mobile devices with 4 to 7 inch LCD panels. Most users and service providers desire DMB service with a larger, higher-quality picture and more varied content. A solution to meet these requirements is to enlarge the data rate while sustaining backward compatibility. These are the main objectives of an AT-DMB system. To satisfy these requirements, a hierarchical modulation scheme was incorporated into the AT-DMB system. In the hierarchical modulation scheme, a QPSK- or BPSK-modulated LP symbol was added to a $\pi/4$ -DQPSK modulated HP symbol as shown in Fig. 1 and (1). The α value, as seen in Fig. 1 and (1), was a predefined constellation ratio with a value of $\{1.5, 2.0, 2.5, 3.0\}$, and β_{HP} and β_{LP} denoted the minimum symbol distances of the HP and LP constellations, respectively. If the α value was increased, more transmission power was allocated to the HP symbol, and if α was decreased, more power went to the LP symbol. Figure 1 only shows the hierarchical modulation procedure of an odd-numbered orthogonal frequency division multiplexing (OFDM) symbol which has a QPSK-modulated LP symbol. However, the procedure for the BPSK-modulated LP symbol case was also same as that shown in Fig. 1, except multiplication of constant phase rotation, $e^{-j\pi/4}$. The complete constellation diagram for even- and odd-numbered OFDM symbols is shown in Fig. 2. The advantage of hierarchical modulation is that this scheme can make both objectives of the AT-DMB system possible, that is, an increased data rate and backward compatibility.

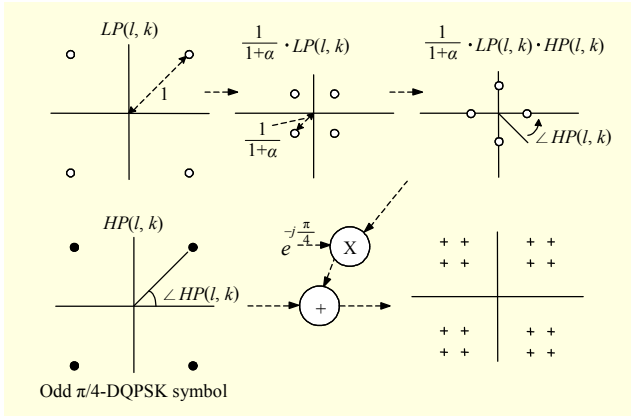


Fig. 1. Hierarchical modulation procedure (LP:QPSK).

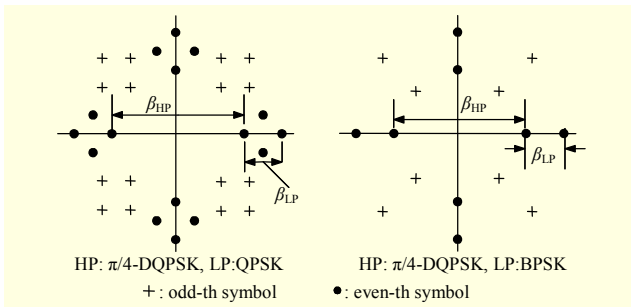


Fig. 2. Complete hierarchical modulated symbol constellation.

Conventional T-DMB receivers take an AT-DMB signal and use its HP stream to decode the transport stream (TS) which contains multimedia service data [4]. On the other hand, AT-DMB receivers can decode both HP and LP streams; therefore, the data rate can be increased.

$$Y(l, k) = \begin{cases} HP(l, k) + \frac{1}{1+\alpha} \cdot LP(l, k) \cdot HP(l, k) \cdot e^{-j\frac{\pi}{4}} & \text{if LP was QPSK modulated} \\ HP(l, k) + \frac{1}{1+\alpha} \cdot LP(l, k) \cdot HP(l, k) & \text{if LP was BPSK modulated, (1)} \end{cases}$$

where α is β_{HP}/β_{LP} , $Y(l, k)$ is data for k -th subcarrier in l -th OFDM symbol, $HP(l, k)$ is HP symbol data, and $LP(l, k)$ is LP symbol data.

Newly added bandwidth can be used for various purposes. For example, the multichannel audio technology can be applied to an AT-DMB audio stream by using additional data bandwidth [5]. Scalable video coding (SVC) technology should also be a very suitable application for AT-DMB systems which use hierarchical modulation. The base layer and enhancement layer of the SVC stream can be sent via the HP stream and the LP stream, respectively, and the AT-DMB receiver can decode both the multichannel audio stream and the SVC video stream by using appropriate synchronization

technology [6].

However, the disadvantage of hierarchical modulation is SNR degradation because the added LP symbols act as noise against HP symbols. The LP symbol distance is smaller than in an HP symbol, so LP performance is worse than that of HP. To mitigate its performance degradation, a turbo decoder is incorporated as an inner error correction code for an LP stream.

Research on AT-DMB systems is ongoing, but most of the major issues have already been resolved. In this work, we present the design of an AT-DMB baseband receiver SoC, and we investigate the feasibility of the AT-DMB system.

The remainder of this paper is organized as follows. Section II describes the design details of the AT-DMB baseband receiver SoC. In section III, the verification and simulation results are described. In section IV, implementation and measurement results of a baseband SoC are discussed. Finally, in section V, we draw some conclusions.

II. Design of AT-DMB Baseband Receiver SoC

A functional block diagram for a baseband receiver SoC and a description of its functional blocks are shown in Fig. 3. The ADC has a 10-bit width and uses a sampling clock of 8.192 MHz. A sampling clock frequency of 8.192 MHz can be used in both a conventional heterodyne RF tuner, which has an intermediate frequency (IF) of 38.912 MHz, and a low-IF tuner, which has an IF of 2.048 MHz. The sampling clock is generated from inside a baseband SoC, and a pulse width modulated (PWM) signal is also generated to control the frequency of the main oscillator. The PWM signal is converted into an analog control signal through a low-pass filter.

The synchronizer consists of a frequency and timing synchronizer. In general, the OFDM scheme has the advantages of a simple equalizer and high data rate. The OFDM scheme can mitigate the inter symbol interference problem by using a cyclic prefix. However, the OFDM scheme is vulnerable to a frequency offset that deteriorates the performance of an OFDM receiver. Most frequency synchronization algorithms for a conventional T-DMB system can also be used for an AT-DMB system. In this work, the integral frequency offset is estimated using the coherent phase bandwidth concept [7], and the fractional frequency offset is estimated using the guard-interval-based algorithm. The normalized frequency offset value, ε , which is calculated using (2), and the frequency offset are corrected using a digitally controlled oscillator (DCO) and a phase rotator as shown in Fig. 3.

$$\varepsilon = \frac{1}{2\pi} \arg \left\{ \sum_{n=-N_G}^{-1} (y_n^* \cdot y_{n+N}) \right\}, \quad (2)$$

where N is the number of fast Fourier transform (FFT) points, y_n

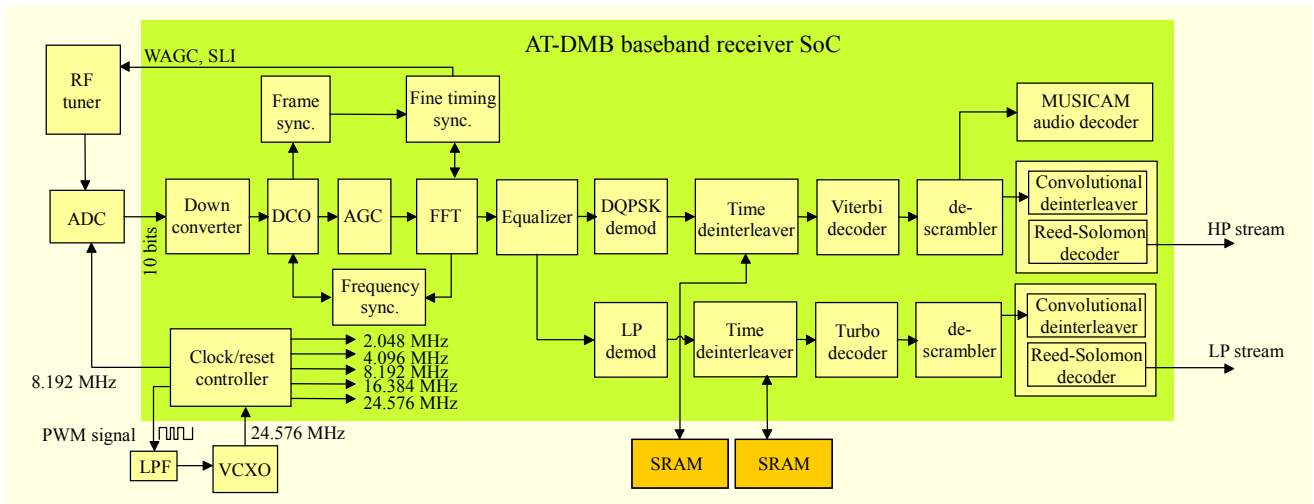


Fig. 3. Functional block diagram for an AT-DMB baseband receiver SoC.

is the received sample value in cyclic prefix, and y_{n+N} is a sample value in symbol data.

The DCO block generates a frequency offset correction signal ($e^{-j2\pi\varepsilon}$) using the estimated frequency offset value, ε . Then, the generated correction signal is multiplied when the received signal is used by the complex multiplier in DCO. The smallest resolution of the frequency synchronizer is 0.001 times the subcarrier spacing. It is well known that the SNR degradation due to a frequency offset is less than 0.1 dB with QPSK modulation if the normalized frequency offset is smaller than 0.01. Therefore, the value of the minimum resolution for a frequency offset correction is set to 0.001 for the frequency synchronizer.

The timing offset is estimated using a channel impulse response (CIR). The CIR can be calculated using a phase reference symbol (PRS). The CIR method requires inverse FFT (IFFT) operations as shown in (3). Using a twisting input and output, the FFT block, which is used for normal OFDM demodulation, is also used for the IFFT function of the timing synchronization:

$$\begin{aligned} CIR &= IFFT(r_k / z_k), \\ \delta &= \underset{k}{Max}(CIR), \end{aligned} \quad (3)$$

where r_k is received PRS, z_k is original PRS, and δ is timing offset.

Synchronization processes were run in a sequential manner, as shown in Fig. 4, because each synchronization algorithm is dependent on the execution order of each algorithm. For example, a timing offset estimation must be run after a frequency offset is compensated completely. If an integral frequency offset is not compensated, the output of the FFT will be a cyclically-shifted version of the transmitted data. Therefore, a timing offset estimation will produce inaccurate

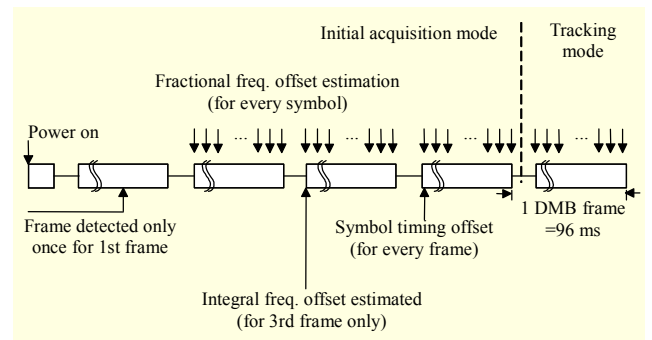


Fig. 4. Timing diagram of synchronization.

results if the frequency offset is not compensated completely.

An accurate timing offset estimation is important because of the moving average process in an equalizer. Even a small timing offset can deteriorate the channel estimation results. The received and sampled OFDM symbol can be expressed as shown in (4), and the corresponding FFT output is shown in (5). In (5), the phases of output data $Y_{n,k}$ are rotated by the amount of timing offset multiplied by the subcarrier index value, that is, $2\pi k\delta$. These phase rotations do not matter for a normal differential demodulation process because the phase differences between adjacent OFDM symbols are not changed even though each symbol is rotated by $2\pi k\delta$. However, these rotated phases are treated as noise during the averaging process of estimated channel coefficients in an equalizer block; otherwise, the averaging process for an estimated channel coefficient can improve the performance [8].

$$\begin{aligned} r_n(m) &= \sum_{k=0}^{N-1} C_{n,k} \cdot e^{j2\pi k \left(\frac{T_s}{N} m + \tau \right)} \\ &= \sum_{k=0}^{N-1} C_{n,k} \cdot e^{j2\pi km/N} \cdot e^{j2\pi k\tau/T_s}, \end{aligned} \quad (4)$$

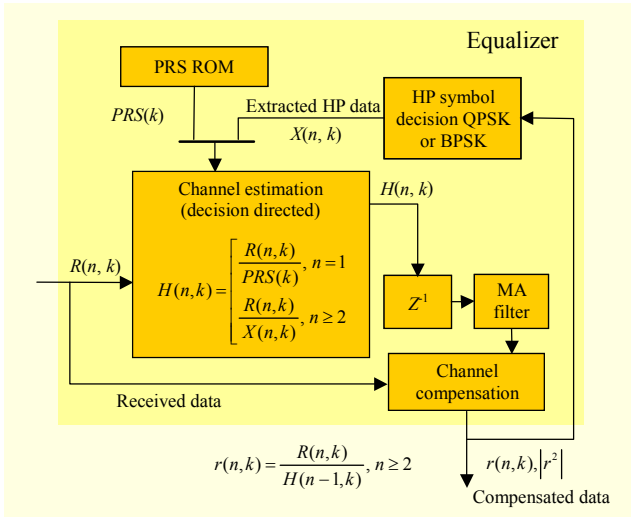


Fig. 5. Equalizer block diagram.

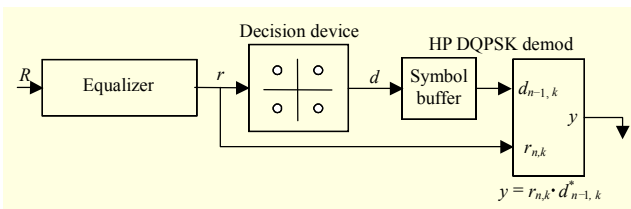


Fig. 6. DQPSK demodulator block diagram.

where $C_{n,k}$ is the k -th subcarrier of n -th transmitted symbol, $r_n(m)$ is sampled data of received symbol, and T_s is sampling time.

$$Y_{n,k} = \frac{1}{N} \sum_{m=0}^{N-1} r_n(m) \cdot e^{-j2\pi mk/N} \quad (5)$$

$$= C_{n,k} \cdot e^{j2\pi k \tau / T_s} = C_{n,k} \cdot e^{j2\pi k \delta},$$

where $Y_{n,k}$ is FFT output data for received symbol.

Synchronization can be separated into two different modes, an initial acquisition mode and a tracking mode. In acquisition mode, the frame timing and frequency offset are estimated and compensated. In tracking mode, only the fractional frequency synchronizer and symbol timing synchronizer are operated, and the varying frequency and timing offset can be tracked.

The FFT block consists of state machine logic, memory, and one butterfly unit. Therefore, computational speed is not fast but has a very small area. One butterfly unit is repeatedly used for the butterfly calculation of the FFT algorithm, and the calculated data is written to the internal memory using an in-place substitution method. The output data of an FFT block has an 8-bit resolution, and the signal power of the FFT output data always remains at a constant level.

The time deinterleaver block in an HP stream deinterleaves the data for a time duration of 384 ms. However, the time deinterleaver in an LP stream deinterleaves the data for a time

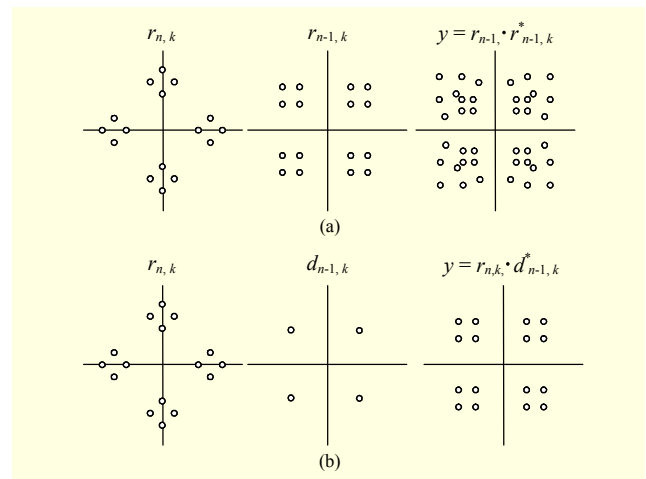


Fig. 7. DQPSK demodulator (a) with and (b) without a decision device.

duration of either 384 ms or 768 ms. If an LP stream uses a QPSK modulation scheme, the time interleaving is the same as that of an HP stream. That is, the deinterleaving time is 384 ms. On the other hand, if an LP stream uses the BPSK modulation scheme, the deinterleaving time can be doubled because the data rate halves. As a result, the fading channel performance can be improved using the same amount of deinterleaving memory. In this work, two external SRAM interfaces are included for the deinterleaving memory as shown in Fig. 3. One SRAM is used for the deinterleaving of 4-bit soft decision Viterbi decoder input data, and the other SRAM is used for 6-bit turbo decoder input metric data.

If SVC technology is used with AT-DMB baseband system, another memory buffer is needed to compensate the interleaving time difference between the HP stream and the BPSK-modulated LP stream. However, we assumed that the video decoder was implemented with PC-based software. Therefore, no additional buffer to synchronize both streams was implemented in the baseband receiver.

The equalization block in Fig. 3 uses a decision-directed method to equalize the output signal of an FFT [9], [10]. A detailed block diagram of the equalizer is shown in Fig. 5. The first channel estimation is conducted using both the received PRS symbol and the stored PRS data as shown in Fig. 5. The estimated channel coefficient is filtered using the moving average filtering block to improve the performance [8]. The next symbol is equalized using the channel estimation coefficient from the previous symbol, and the received HP data $X(n, k)$ are extracted from compensated symbol $r(n, k)$. The extracted HP data, $X(n, k)$, are used as known data of the input symbol. Decision-directed channel estimation is conducted using input symbol $R(n, k)$ and extracted HP symbol data $X(n, k)$. The $|r^2|$ signal represents the envelope of the output

Table 1. E_b/N_0 value comparison for $BER=10^{-4}$ (coded, AWGN).

	T-DMB	Without decision device	With decision device
FIC (Viterbi)	1.75 dB	2.96 dB	2.5 dB
MSC (RS, prot. level=4)	5.1 dB	6.99 dB	6.63 dB

Table 2. Turbo decoder code rate and block size.

Type	Protection level	Code rate	Code block size
MSC	1-C	1/4	3,072K + 768L bits
	2-C	1/3	
	3-C	2/5	
	4-C	1/2	
FIC	-	1/3	3,072 bits

signal $r(n, k)$ which was used by the LP symbol demapper to decide the LP symbol.

The differential QPSK demodulator is almost the same as that of a conventional T-DMB receiver, except the decision device is needed before the differential decoding as shown in Fig. 6.

If there is no decision device, the DQPSK-demodulated symbols are spread as shown in Fig. 7(a), and the performance of the differential demodulator deteriorates. However, if the DQPSK demodulator adopts a decision device, the constellation of the differential demodulator output is not spread, as shown in Fig. 7(b), and the performance is almost the same as that of a conventional T-DMB, which does not use hierarchical modulation.

The performance difference between the schemes in Fig. 7(a), Fig. 7 (b), and a conventional T-DMB was simulated under a coded AWGN channel environment, and the results are shown in Table 1. Table 1 shows the E_b/N_0 values at the crossing point of $BER=10^{-4}$ level.

The performance of the LP stream is worse than that of the HP stream because of the shorter symbol distance. Therefore, a turbo code was adopted for the inner error correction system of the LP stream instead of a Viterbi decoder. The outer code of the LP stream is the same as that of the conventional T-DMB system, which consists of a Reed-Solomon (RS) decoder and a convolutional deinterleaver. The turbo code, which was implemented in an AT-DMB baseband SoC, is a duo binary circular recursive systematic convolution code [11]. The rate control was conducted using four different puncturing levels as shown in Table 2.

For the fast information channel (FIC) in an LP stream, the code block length is 3,072 bits, which means all of the FIC data for one frame is encoded using a single code block. In the case

of the main service channel (MSC), the code block length is calculated as

$$\text{Coded block length} = 3,072K + 768L. \quad (7)$$

At first, the information bits are encoded into K code blocks of 3,072 bits, and the remaining bits are encoded as L code blocks of 768 bits. The implemented turbo decoder utilizes the log2MAP algorithm [12], and the turbo decoder iterates 6 times to correct the errors in the code block. More iterations provide more coding gain, but the performance enhancement is almost saturated at 6 to 7 iterations. The Viterbi decoder, which is used for the HP stream, has the parameters of a 4-bit soft-decision metric and a truncation length of 64. The soft-decision metric can improve the performance of the Viterbi decoder, but the performance improvement is almost saturated at 4 soft-decision bits, and the truncation length is known to be sufficient using a value 6 times that of the maximal memory order of the convolution encoder.

An RS decoder has the specification parameters of 204, 188, and $t=8$. This means that 188 bytes of a message are encoded. As a result, 204 bytes of output are generated. Therefore, an RS code can correct a maximum of 8 bytes of error within one TS packet. The modified Euclidian algorithm was used to find the error polynomials, and the Chien search algorithm was used to find the error locations within the error polynomials.

III. Design Verification and Performance Simulation

We simulated the AT-DMB baseband receiver HDL design to verify its functionality and performance using a hardware accurate c-model. The implementation parameters which applied to both the c-model and hardware design are summarized in Table 3.

A real transmission signal was captured using a commercial RF tuner and ADC components, and both the c-model and RTL design were simulated using a real captured transmission signal. All of the functional block outputs of Fig. 3 were compared and verified using the c-model; thus, we could ensure that the c-model and hardware design would be exactly the same.

As shown in Fig. 8 and Table 4, the AT-DMB system can achieve almost double the data rate compared to a conventional T-DMB system with a small sacrifice in performance. The BER performance of the AT-DMB system was worse than in the conventional T-DMB system as shown in Fig. 8; however, the data rate increased as shown in Table 4. If we use BPSK modulation in the LP stream, the HP stream performance can be increased because unwanted noise effect due to the BPSK modulated LP symbol is smaller than the case of LP uses QPSK modulation. For further information, the carrier-to-noise-ratio analysis of the hierarchical modulation scheme was

Table 3. Summary of implementation parameters.

Block	Parameter descriptions
System parameters	Bandwidth = 2.048 MHz Subcarrier space (Δf)=1 kHz, 2048 point FFT
ADC	10 bits
Synchronizer	Timing and frequency synchronizer enabled
Reed-Solomon decoder	(204, 188, $t=8$) Chien search, modified Euclidean algorithm
Viterbi decoder	(133, 171, 145, 133) 4-bit soft-decision metric, trace-back depth=64
Turbo decoder	Double binary circular recursive systematic convolutional (CRSC) code [11] log2MAP algorithm, iterations = 6
LP depuncture	Code rate = 1/4, 1/3, 2/5, 1/2 for protection levels 1-C, 2-C, 3-C, 4-C, respectively
Equalizer	Decision directed equalizer with channel coefficient average filtering
Demodulator	Hierarchical modulation HP: $\pi/4$ -DQPSK / LP: QPSK or BPSK
Time deinterleaving	HP: 384 ms / LP: 768 ms

Table 4. Maximum bit rate of AT-DMB.

	Prot. level	LP		HP		Overall bit rate (kbps) HP, LP:QPSK (HP,LP:BPSK)
		Code rate	Bit rate*(kbps) LP:QPSK (LP:BPSK)	Code rate	Bit rate* (kbps)	
M S C	1	1/4	528 (264)	1/4	528	1056 (7932)
	2	1/3	704 (352)	3/8	792	1496 (1144)
	3	2/5	821 (412)	1/2	1056	1877 (1468)
	4	1/2	1056 (528)	3/4	1584	2640 (2112)
FIC	-	1/3	32 (16)	1/3	32	64 (48)

*Exclude TS packet sync. byte and RS encoder redundancy

However, the bit rate of the LP stream was half the bit rate when QPSK modulation was used. BPSK modulation for an LP stream has another benefit in terms of time diversity because the time interleaving depth can be increased to 768 ms with the same memory capacity. Therefore, the BPSK modulation scheme is suitable for a mobile receiving environment of an AT-DMB LP stream.

presented in [13].

The LP stream performance can be dramatically improved using the BPSK modulation scheme as shown in Fig. 8.

VI. AT-DMB Baseband Receiver Implementation

The design parameters and architecture of the implemented AT-DMB baseband receiver are shown in Fig. 3 and Table 3.

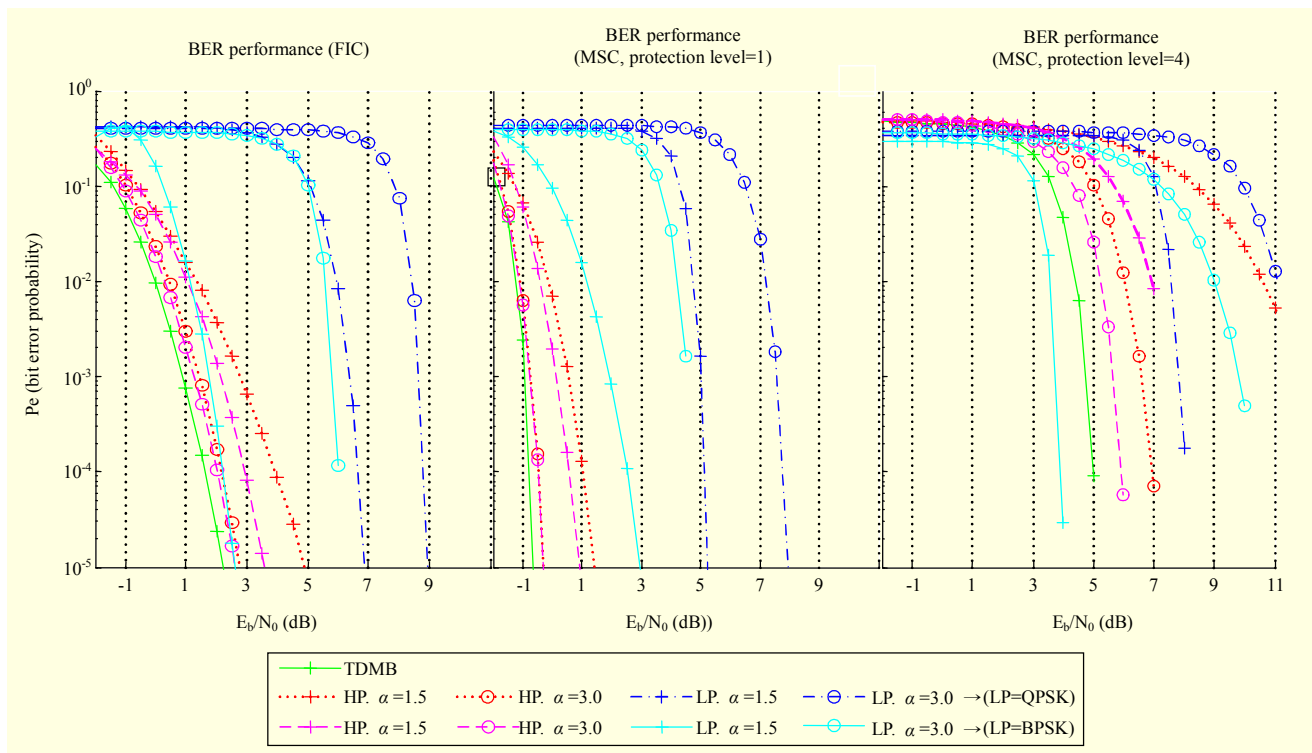


Fig. 8. Simulation results of BER performance of AT-DMB baseband receiver SoC.

The baseband SoC was fabricated using 0.13 μm 1-poly 8-metal technology, and the package has 256 pins including a power supply and debugging interface pins. The die area of the fabricated SoC chip is 5 mm \times 5 mm as shown in Fig. 9.

Detailed implementation results are summarized in Table 5.

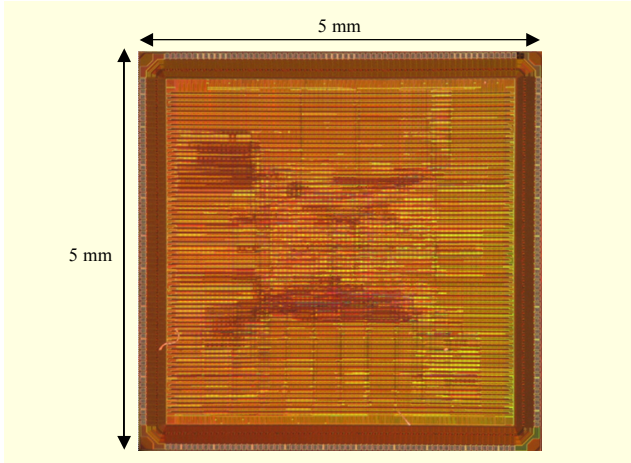


Fig. 9. Photograph of the fabricated SoC chip.

Table 5. Summary of implementation results.

Block	Memory (bit)	Equivalent gate count (inc. memory)	%
AGC	0	2,610	0.2%
Equalizer	55,296	57,423	4.4%
Frequency deinterlv.	36,864	65,254	5.0%
Demodulator	66,432	53,508	4.1%
Time deinterlv.	0	78,304	6.0%
FFT	114,688	78,305	6.0%
Conv. deinterlv. (HP/LP)	20,480	52,202	4.0%
Descrambler (HP/LP)	0	20,880	1.6%
RS decoder (HP/LP)	6,528	23,490	1.8%
Synchronizer	109,568	53,508	4.1%
Turbo decoder	497,664	525,948	40.3%
Viterbi decoder	12,544	71,762	5.5%
Miscellaneous function block	0	221,890	17.0%
Total	920,064	1,305,084	100%

Table 6. Power dissipation measurement results.

Block	Current (mA)	Supply (V)	Power (mW)
Core	25	1.8	45
I/O	1.65	3.3	5.4
Total power dissipation			50.4

The fabricated AT-DMB baseband SoC shows successful operation with power dissipation of 50.4 mW under the condition of 24.576 MHz operating clock and the supply voltages given in Table 6.

V. Conclusion

This work reports the first implementation results of an AT-DMB baseband SoC, and with the results of this work, we can conclude the following.

The AT-DMB baseband system architecture is appropriate for implementation with hardware SoCs; however, some special considerations that are mentioned in this paper must also be included. The AT-DMB system can achieve double the data rate with a sacrifice of a small amount of SNR degradation, and the baseband hardware SoC can be implemented with an approximately 1.3 million equivalent gate count and 50 mW power dissipation using 0.13 μm technology.

References

- [1] ETSI, ETSI EN 300 401, *Radio Broadcast Systems; Digital Audio Broadcasting (DAB) to Mobile, Portable and Fixed Receivers*, European Telecommunications Standards Institute, May 2001.
- [2] ETSI, ETSI TS 102 428, *Digital Audio Broadcasting DMB Video Service; User Application Specification*, European Telecommunications Standards Institute, 2005.
- [3] B. Sostawa and J. Speidel, "Investigations on Bit Error Performance for Video over DAB," *IEEE Trans. Broadcast.*, vol. 44, Dec. 1998, pp. 445-448.
- [4] G.S. Lee et al., "A Novel Method for Inserting an MPEG-2 TS into Ensemble in a DMB Transmission System," *ETRI J.*, vol. 26, no. 6, Dec. 2004, pp. 653-656.
- [5] J. I. Seo et al., "Multi-channel Audio Service in a Terrestrial-DMB System Using VSLI-Based Spatial Audio Coding," *ETRI J.*, vol. 27, no. 5, Oct. 2005, pp. 635-638.
- [6] K.D. Seo, S.H. Jung, and J.S. Kim, "Efficient Media Synchronization Mechanism for SVC Video Transport over IP Networks," *ETRI J.*, vol. 30, no. 3, June 2008, pp. 441-450.
- [7] K.J. Bang et al., "A Coarse Frequency Offset Estimation in an OFDM System Using the Concept of the Coherence Phase Bandwidth," *IEEE Trans. Commun.*, vol. 49, no. 8, Aug. 2001, pp. 1320-1324.
- [8] S.D. Ha et al., "Detection of Hierarchically-Modulated Data for Advanced T-DMB Receivers," *IEEE Int. Conf. Consum. Electron.*, June 2008, pp. 1-2.
- [9] J.H. Kim et al., "Coherent Detection for T-DMB Receiver in Hierarchical Modulation Mode," *IEEE Trans. Consum. Electron.*, vol. 53, no. 2, May 2007, pp. 294-299.
- [10] S.H. Kim et al., "Design of the Channel Estimation Algorithm for

Advanced Terrestrial DMB System,” *IEEE Trans. Broadcast.*, vol. 54, no. 4, Dec. 2008, pp. 816-820.

- [11] J.T. Bae et al., “The Performance Analysis of Advanced T-DMB Using Unequal Error Protection System and Hierarchical Modulation,” *IEEE Int. Conf. Commun. Electron.*, June 2008, pp. 288-293.
- [12] I.S. Jeon et al., “An Efficient Turbo Decoder Architecture for IMT2000,” *IEEE Int. Conf. VLSI and CAD*, Oct. 1999, pp. 301-304.
- [13] H. Jiang and P.A. Wilford, “A Hierarchical Modulation for Upgrading Digital Broadcast Systems,” *IEEE Trans. Broadcast.*, vol. 51, no. 2, June 2005, pp. 223-229.



Joohyun Lee received the MS degree in electrical engineering from Pohang University of Science and Technology (POSTECH), Korea, in 1998. In 1998, he joined the advanced DRAM design team of Hynix, Korea. Since 2000, he has been with ETRI, Korea. His research interests include synchronization of OFDM receivers, multimedia broadcasting, and LTE-based FemtoCell technology.



Hyuk Kim was born in Gwangju, Korea. He received the MS degree in electronic engineering from Chonnam National University, Korea, in 1999. In 1999, he joined the Telecommunication Digital Circuit Team of ETRI, Korea. Currently, he is a senior research member of the Application SoC Design Team of ETRI, and his research interests include channel coding, network coding, and LTE-based FemtoCell technology.



Jinkyu Kim received the MS degree in electrical engineering from Chungbuk National University, Korea, in 2000. In 2000, he joined ETRI, Korea, where he is currently a senior research member. His research interests include error control systems and 3G LTE systems.



Bontae Koo received the BS and MS degrees in electrical engineering from Korea University, in 1989 and 1991, respectively. He was with Hyundai Electronics in Korea from 1991 to 1997 and ASPEC in San Jose, USA, from 1997 to 1999. He joined ETRI, Korea, in 1999. Currently, he serves as the team leader for the Application SoC Development Team.



Nak-Woong Eum received the BS degree in Electronic Engineering from Kyungbook National University, Korea, in 1984 and the MS and PhD degrees in electrical engineering from KAIST, Korea, in 1987 and 2001, respectively. Since 1987, he has been working with ETRI, Daejeon, Korea, as a principal member of engineering staff, where he is currently the director of the System-on-Chip Research Department. His current research interests include embedded processor technology, mobile multimedia system, and System-on-Chip design methodology.



Hyuckjae Lee received the BS degree in electronic engineering from Seoul National University, Korea, in 1970, and the PhD in electrical engineering from Oregon State University, Corvallis, in 1982, where he specialized in electromagnetic fields and microwave engineering. Since 1983, he has been with the Radio Technology Department of ETRI and working in the fields of radio technology, IMT2000, broadcasting technology, and satellite communications systems. He is currently a professor of Korea Advanced Institute of Science and Technology (KAIST).